The *Forbidden* Abundance of Oxygen in the Sun

Carlos Allende Prieto and David L. Lambert

McDonald Observatory and Department of Astronomy, The University of Texas, Austin, TX 78712-1083, USA

and

Martin Asplund

Uppsala Astronomiska Observatorium, Box 515, Uppsala 75120, SWEDEN

Received _____; accepted _____

Submitted to ApJL

ABSTRACT

We reexamine closely the solar photospheric line at 6300 Å, which is attributed to a forbidden line of neutral oxygen, and is widely used in analyses of other late-type stars. We use a three-dimensional time-dependent hydrodynamical model solar atmosphere which has been tested successfully against observed granulation patterns and an array of absorption lines. We show that the solar line is a blend with a Ni I line, as previously suggested but oftentimes neglected. Thanks to accurate atomic data on the [O I] and Ni I lines we are able to derive an accurate oxygen abundance for the Sun: $\log \epsilon(\mathrm{O}) = 8.69 \pm 0.05$ dex, a value at the lower end of the distribution of previously published abundances, but in good agreement with estimates for the local interstellar medium and hot stars in the solar neighborhood. We conclude by discussing the implication of the Ni I blend on oxygen abundances derived from the [O I] 6300 Å line in disk and halo stars.

Subject headings: Sun: abundances — Sun: photosphere

1. Introduction

The cosmic abundance of oxygen is an important number in a wide variety of scenarios. Several debates have over the years focussed on disagreements about the oxygen abundance of stars, and disparities between estimated abundances for different kinds of astronomical objects. For example, there is a long history of using hot stars as tracers of the galactic radial variation of the oxygen abundance, but only very recently have the stellar abundances seemed to agree with the results derived from emission lines in H II regions (Rolleston et al. 2000). Currently, the study of metal-poor stars is particularly polemical. A group of astronomers defends a monotonic increase of the oxygen-to-iron ratios (i.e., [O/Fe]) with

lower iron abundances (see, e.g., Israelian et al. 2001; Boesgaard et al. 1999), whereas a second group tends to prefer an essentially constant [O/Fe] for stars with [Fe/H] $\lesssim -1$ (see, e.g., Carretta, Gratton & Sneden 2000; Nissen, Primas & Asplund 2000). The discrepancy for metal deficient stars may be connected to the use of different indicators of the oxygen abundances and, ultimately, caused by deficiencies in the modeling of the spectra.

The solar oxygen abundance is not free from debate. In fact, the solar controversy and that in metal-poor stars could be related. The most popular indices of the oxygen abundance in cool stars are i) the [O I] forbidden lines at 6300 and 6363 Å; ii) the OH lines in the UV and IR; and iii) the O I triplet at about 7773 Å[1]. In the solar case, the forbidden lines and the OH lines tend to provide higher abundances, by about $0.1 - 0.2$ dex, than the O I 7773Å triplet, when allowance for departures from Local Thermodynamic Equilibrium (LTE) in the formation of the triplet is made.

None of the indicators of the solar oxygen abundance is free from suspicion. The popular [O I] lines are threatened by the presence of blends (Lambert 1978). The O I 7773 Å triplet likely suffers important departures from LTE (see e.g. Kiselman 1993; Takeda 1994; Reetz 1999a,b). The OH lines are particularly sensitive to temperature, and therefore compromised by deficiencies in the model atmospheres (e.g., Sauval et al. 1984; Asplund & García Pérez 2001). In addition, all lines are affected by surface inhomogeneities (granulation) that are ignored by classical model atmospheres (Kiselman & Nordlund 1995).

[1]Unfortunately, weaker (forbidden and allowed) O I lines in the optical and near-IR solar spectrum appear to be either heavily blended with several (some times unknown) other features (e.g. 5577.3, 6156.8, 6158.2, 9741.5, 11302.2 Å), lack atomic data (e.g. 9760.7 Å),or are affected by a large uncertainty in the continuum location (e.g. 8446.3, 9265.99 Å), or suffer some of these problems simultaneously, occasionally in combination with serious departures from LTE (e.g. 8446.8 Å).

Some lines are likely afflicted by several errors acting in concert, for example, the OH UV lines may be affected not only by model atmosphere uncertainties but also by significant departures from LTE, and the uncertainties in the opacities in that spectral region (Hinkle & Lambert 1975; Bell, Balachandran & Bautista 2001; Asplund & García Pérez 2001).

We reexamine the solar [O I] 6300 Å line using synthetic spectra based on a three-dimensional hydrodynamical model atmosphere, and allowing for the Ni I blend. A principal advantage of the [O I] line is that departures from LTE should be very small. A disadvantage is that the line is weak and, therefore, susceptible to blends. As discussed by Lambert (1978), the line at 6300 Å is blended with a Ni I feature, while that at 6363 Å is affected by a CN line. We consider only the 6300 Å line because the blending Ni I line makes a smaller contribution to the solar line than does the CN line to the 6363 Å line (Reetz 1999a), the 6363 line is located in the middle of a broad Ca I auto-ionization line and, as discussed for OH, molecular features are particularly sensitive to the details of the temperature structure. The next section describes the basic ingredients involved in the analysis, §3 is devoted to the comparison with the solar flux spectrum to derive the photospheric oxygen abundance, and §4 is a brief summary of the results.

2. Model atmospheres and line synthesis

We made use of a 3D time-dependent hydrodynamical simulation of the solar surface calculated by Asplund et al. (2000), and based on the compressible radiative hydrodynamical code described by Stein & Nordlund (1998). The equations of mass, momentum, and energy conservation together with the simultaneous treatment of the 3D radiative transfer equation were solved on a Eulerian grid with $200 \times 200 \times 82$ points to represent $(6 \times 6 \times 3.8) \times 10^3$ km in the solar surface, with about 10^3 km above continuum optical depth unity. For more details we refer the reader to Asplund et al. (2000) and

references therein.

The calculated flux profiles for the [O I] and Ni I lines at 6300 Å from the 3D simulation are based on a sequence of 50 minutes, taking a snapshot every 30 seconds. The integration over the disk used 4×4 angles, and took into account the solar surface rotation as a solid body ($v_{\rm rot} \sin i \simeq 1.9$ km s^{-1}). The Uppsala synthesis package (Gustafsson et al. 1975 with subsequent updates) was the source of the continuum opacities, partition functions, ionization potential and other basic data for the line synthesis as well as for the simulation. Collisional broadening by hydrogen atoms was considered following the van der Waals formula, but is essentially irrelevant for the extremely weak lines considered (equivalent widths $\lesssim 5$ mÅ). Natural broadening, also irrelevant, was included, using data from the Vienna Atomic Line Database (VALD; Kupka et al. 1999). Reduction of the partial pressure of oxygen through CO formation is included with the carbon abundance put at $\log \epsilon({\rm C}) = 8.52$; though the effect on the number density of O I is $\leq 5\%$. Our assumption of LTE for the [O I] line formation is supported by our own NLTE calculation for various 1D model solar atmospheres. It must be stressed that the line profiles are predicted *ab initio*, i.e., microturbulence and macroturbulence are not invoked and adjusted to fit these or other lines. Convective velocity fields and thermal broadening are provided by the model.

Our goal was to determine the best fit to the solar 6300 Å feature using the known atomic parameters for the [O I] and Ni I lines. The laboratory wavelength of the [O I] line was measured by Eriksson (1965) as 6300.304 ± 0.002 Å. The transition probability for the [O I] line is dominated by the magnetic dipole contribution with a minor (0.3%) electric quadrupole contribution. We adopt Storey & Zeippen's (2000) relativistic calculation of the magnetic dipole contribution, and following them include the electric quadrupole contribution from Galavís, Mendoza, & Zeippen (1997) to obtain $\log gf = -9.717$ with an accuracy of a few per cent. Inclusion of relativistic corrections reduced the value by less

than 2 %. The $\log gf$ has changed little over the years; Lambert (1978) suggested -9.75, after comparison of laboratory and older theoretical determinations.

The blending Ni I line's wavelength was measured as 6300.339 Å by Litzén, Brault, & Thorne (1993) with an estimated uncertainty of 2 to 3 mÅ. Litzén et al.'s energy levels derived from their extensive reinvestigation of the Ni I spectrum predict 6300.342 Å for the line. The NIST web database gives 6300.343 Å, as calculated from the energy levels of Sugar & Corliss (1985). Litzén et al. did not report measurable isotopic splitting and, therefore, we neglect isotopic (and hyperfine) splitting. We have adopted 6300.339 Å as the rest wavelength of Ni I line. The $\log gf$ for the Ni I line is uncertain. There are seemingly no laboratory measurements for this line. The energy levels clearly show that LS-coupling is an inappropriate assumption from which to derive the solar gf-value using Ni I lines of the same and similar multiplets. Indeed, Moore's (1959) classification gives the transition as y $^3D^\circ_1$ - e $^3P_0$ but severe configuration interaction renders these misleading labels. Litzén et al. show that the dominant (90%) contribution to the upper term is not from the ^{3}P term but from a ^{1}S term, and while the leading contribution to the lower term is from the ^{3}D term there is an appreciable contribution (34%) from other terms. These contributions differ for different levels of the lower and upper terms. We treat the product $gf\epsilon$(Ni) as a free parameter.

3. Comparison with the observed spectrum

We have confronted our calculated profiles with the FTS solar flux spectrum published by Kurucz et al. (1984). The resolving power is about half a million, and the signal-to-noise ratio amounts to several thousand, making these data adequate for studying the [O I] feature at 6300 Å. Allende Prieto & García López (1998) checked that the wavelength scale of the atlas is very accurate. It has been corrected for the Earth-Sun velocity, but not

for the gravitational redshift, which amounts to 633 m s^{-1} for the photospheric spectrum intercepted at Earth.

Two strong lines (Si I 6299.6 Å and Fe I 6301.5 Å) depress the continuum in the immediate vicinity of the [O I] - Ni I blend, but have a negligible effect on the shape of the observed blend. Other weaker lines might be present closer to the blend, as reflected by the slightly irregular shape of the spectrum, discouraging the individual modeling of all lines, but rather suggesting a zeroth-order correction to the continuum level, which becomes one of the fitting parameters. As the 3D models predict the convective line asymmetries and shifts for weak neutral lines to well within 0.1 km s^{-1} ($\approx$ 0.002 Å; Asplund et al. 2000), the shifts - absolute and differential - of the oxygen and nickel lines from the laboratory wavelengths cannot be adjusted. Therefore, the only parameters we can tune to match the predicted profile to the observed profile are the continuum level, the oxygen abundance, and the product $gf\epsilon$(Ni). The optimization of the fit was accomplished using the slow-but-robust amoeba algorithm based on the Nelder-Mead simplex method (Nelder & Mead 1965; Press et al. 1986).

Figure 1a shows the agreement between the observed profile (filled circles) and that calculated with the 3D model atmosphere (solid line). The oxygen and nickel lines are represented with dashed lines. Adopting a signal-to-noise-ratio (S/N) of 2100, estimated from the region between 6303.10 and 6303.25 Å, we choose to minimize the reduced χ^2 in the region between 6300.15–6300.40 Å to avoid apparent blends outside the selected region, which leads to a multiplicative correction to the local continuum level in the solar atlas of $C = 1.0083$. Alternative reasonable choices of C do not change the retrieved oxygen abundance by more than 0.02 dex (see below). A change as small as 0.005 Å in any direction in the wavelengths of the oxygen or nickel lines would degrade the final χ^2 of an optimal fit.

The reduced χ^2 (34 frequencies and 3 degrees of freedom) for the flux between 6300.15

and 6300.40 Å is 0.30, and the probability for this to happen by chance is $P = 5 \times 10^{-5}$. We stress that we have corrected for the Sun-Earth gravitational redshift (633 m s^{-1}), but no arbitrary shifts have been allowed for the oxygen, nor for the nickel lines, nor for both as a pair. No macro-turbulence or micro-turbulence enter the fit. The effective temperature or, equivalently, the entropy at the lower boundary of the simulation box, was carefully adjusted prior to starting the simulation. The temporal average of $T_{\rm eff}$ from the simulation is 5767 ± 21 K, where the quoted error is the standard deviation for the 100 snapshots. The adopted surface gravity is $\log g = 4.437$ (cgs). The uncertainties in the solar gravity, effective temperature, and chemical composition have a negligible impact on the fit.

External uncertainties inherent in the adopted set of continuum opacities, partition functions, equation of state, etc. are considered as part of our systematic errors. From tests with different synthesis codes and previous experience, we expect these not to exceed 0.02 dex. The estimated uncertainty in the theoretical value adopted for the transition probability of the forbidden line adds a contribution of similar size. An uncertainty in the wavelength of the Ni I of ± 0.003 Å translates to an error in the oxygen abundance of $^{+0.02}_{-0.02}$ dex and $^{-0.03}_{+0.04}$ in $\log[gf\epsilon(\mathrm{Ni})]$. The same shifts in the wavelength of the [OI] line would produce a change of $^{+0.04}_{-0.03}$ dex in the oxygen abundance and $^{-0.15}_{+0.10}$ dex in $\log[gf\epsilon(\mathrm{Ni})]$. Simultaneous shift of the rest central wavelengths of both lines by ± 0.003 Å would induce changes to the determined abundance of oxygen by $^{+0.04}_{-0.05}$ dex, and $^{-0.18}_{+0.12}$ dex in $\log[gf\epsilon(\mathrm{Ni})]$.

We find $\log \epsilon(\mathrm{O}) = 8.69 \pm 0.05$ dex. Fig. 2 shows the projection onto the $C - \log \epsilon(\mathrm{O})$ plane of the reduced χ^2. The scale for both the gray-scale and the contours is logarithmic and, therefore, the units in the gray-scale code bar are dex.

Our evaluation of the Ni I line is equivalent to $\log[gf\epsilon(\mathrm{Ni})] = 3.94$. Adopting the solar Ni abundance from Grevesse & Sauval (1998), we obtain $\log gf$ = -2.31 for the Ni I line, which compares with $\log gf$ = -1.74 computed by Kurucz & Bell (1995). Figure 1b shows

the best fit obtained assuming the solar feature at 6300 Å is entirely produced by the oxygen forbidden line: the abundance derived would be $\log \epsilon(\mathrm{O}) = 8.82$ dex, which allowing for the differences in the adopted $\log gf$s and the correction due to consideration of 3D ($\simeq 0.08$ dex), is in perfect agreement with previous results based on 1D model atmospheres and neglect of the Ni I blending line. If a redshift of about 10 mÅ (476 m s^{-1}) is applied to the predicted profile, the fit to the observations is obviously improved, but we argue that such a shift far exceeds known sources of wavelength-related errors.

Unpublished measurements of the Ni I line report the detection of five isotopic components (referee's private communication). Adopting those isotopic shifts and solar system abundance ratios (Anders & Grevesse 1989), we find a slightly worse fit to the observed feature (reduced $\chi^2 = 0.45$), and our estimate of the solar oxygen abundance increases by 0.01 dex. Kurucz lists 70 weak CN lines between 6300.0 and 6300.6 Å[2], which should be responsible for at least part of the continuum depression that we find. A significant unrecognized blend or blends in the observed feature would further lower the oxygen abundance, although the extremely good fit that we find constrains tightly such possibility.

Reetz (1999a,) analyzed the 6300 Å line using empirical 1D model atmospheres and high S/N spectra of the solar disk-center and limb. The observed profile was fitted not only by adjusting the contributions of the [O I] and Ni I lines but also by including microturbulence and macroturbulence. With the Holweger-Müller (1974) atmosphere, the oxygen abundance including a Ni I contribution, Reetz obtained $\log \epsilon(\mathrm{O}) = 8.81$ from fits to the center and the limb spectra. His value on correction to our adopted gf-value for the [O I] line corresponds to $\log \epsilon(\mathrm{O}) = 8.75$, a difference of 0.06 dex from our result. This difference could be bridged by adopting another choice for the empirical model – see Reetz

[2]http://kurucz.harvard.edu

(1999a, Table 3.3). The Ni I line's gf-value was set by considering other but similar lines and the adjustments to the Kurucz gf-values needed to fit the solar lines. Reetz apparently fitted the 6300 Å line profile equally well with and without the Ni I line and, therefore, his preferred lower oxygen abundance is based on the argument used to set the Ni gf-value ($\log gf = -1.95$). In our case, the line profile is used to set the Ni I line's contribution.

4. Summary and conclusions

The photospheric oxygen abundance we determine from the 6300 Å feature, $\log \epsilon(\mathrm{O}) = 8.69 \pm 0.05$ dex, is at the lower end of the distribution of oxygen abundances previously published. This lower value results partly from adoption of the recent relativistic calculation of the transition probability, but is primarily the result of two factors: (i) the use of the 3D hydrodynamical model atmosphere instead of the Holweger-Müller model ($\simeq -0.08$ dex), and (ii) an accounting for the contribution of the Ni I line ($\simeq -0.13$ dex). The lower oxygen abundance is consistent with the oxygen abundances found in the local interstellar medium when adopting an oxygen gas-to-dust ratio of ~ 2 (Meyer, Jura & Cardelli 1998), and in the photospheres of hot stars in the solar neighborhood (e.g. Cunha & Lambert 1994; Kilian, Montenbruck, & Nissen 1994), both of which typically fall in the range $8.65 - 8.70$ dex.

As [Ni/Fe] $\simeq 0$, and oxygen is known to be relatively more abundant at lower metallicities, the importance of the nickel line in the 6300 Å blend will decrease in metal-poor stars, becoming negligible below [Fe/H] $\simeq -1$. However, it is important to note that the common practice of using a scale relative to the solar abundances would affect the shape of any possible trend of [O/Fe] in the range $-1 \leq$ [Fe/H] ≤ 0. In particular, the nearly constant [O/Fe] in stars with $-0.3 \leq$ [Fe/H] $\leq +0.3$ found by Nissen & Edvardsson (1992) is likely an artifact. Because the contribution of the Ni line is negligible below

[Fe/H] < -1, our findings do not affect how the O/Fe ratio changes at low metallicities and, therefore, do not resolve the controversy mentioned in the Introduction. Nonetheless, acknowledging the presence of the Ni I blend in the solar line has the effect of increasing [O/Fe] by roughly 0.13 dex in stars with [Fe/H] < -1.

This *Letter* exemplifies the importance of detailed line profiles and accurate wavelength scales in chemical analyses of stars from spectra, as well as the need for hydrodynamical model atmospheres in fine analyses of stellar spectra.

We thank Poul Nissen for inquiring about the Ni I line's effect on oxygen abundance determinations, and both Sveneric Johansson and the anonymous referee for alerting us to the reinvestigations of the Ni I spectrum. This work has been possible with the financial help of the US National Science Foundation (grant AST-0086321), the Robert A. Welch Foundation of Houston (Texas), and the Swedish Natural Science Foundation (NFR F990/1999).

REFERENCES

Allende Prieto, C. & García López, R. J. 1998, A&AS, 129, 41

Anders, E., & Grevesse, N. 1989, Geochim. Cosmochim. Acta, 53, 197

Asplund M., García Pérez A.E., 2001, A&A, 372, 601

Asplund, M., Nordlund, Å., Trampedach, R., Allende Prieto, C., & Stein, R. F. 2000, A&A, 359, 729

Bell, R. A., Balachandran, S. C., & Bautista, M. 2001, ApJ, 546, L65

Boesgaard, A. M., King, J. R., Deliyannis, C. P., & Vogt, S. S. 1999, AJ, 117, 492

Carretta, E., Gratton, R. G., & Sneden, C. 2000, A&A, 356, 238

Cunha, K. & Lambert, D. L. 1994, ApJ, 426, 170

Eriksson, K. B. S. 1965, Ark. Fys. 30, 199

Galavís, M. E., Mendoza, C., Zeippen, C. J. 1997, A&AS, 123, 159

Grevesse, N., & Sauval, A. J. 1998, Space Science Reviews, 85, 161

Gustafsson, B., Bell, R. A., Eriksson, K., & Nordlund, A. 1975, A&A, 42, 407

Hinkle, K. H. & Lambert, D. L. 1975, MNRAS, 170, 447

Holweger, H., & Müller, E. A. 1974, Solar Phys. 39, 19

Israelian, G., Rebolo, R., García López, R.J., Bonifacio, P., Molaro, P., Basri, G., Shchukina, N. 2001, ApJ, 551, 833

Kilian, J., Montenbruck, O., & Nissen, P. E. 1994, A&A, 291, 757

Kiselman, D. 1993, A&A, 275, 269

Kiselman, D. & Nordlund, A. 1995, A&A, 302, 578

Kupka, F., Piskunov N., Ryabchikova T. A., Stempels, H. C., & Weiss, W. W. 1999, A&AS, 138, 119

Kurucz, R.L., & Bell, B. 1995, Kurucz CD-ROM No.23 (Harvard-Smithsonian Center for Astrophysics)

Kurucz, R. L., Furenlid, I., & Brault, J. 1984, National Solar Observatory Atlas, (Sunspot, New Mexico: National Solar Observatory)

Lambert, D. L. 1978, MNRAS, 182, 249

Litzén, U., Brault, J.W., & Thorne, A.P. 1993, Phys. Scr. 47, 628

Meyer, D. M., Jura, M., & Cardelli, J. A. 1998, ApJ, 493, 222

Moore, C. E. 1959, NBS Tech. Note No. 56

Nelder, J. A., & Mead, R. 1965, Comput. J., 7, 308

Nissen, P. E., & Edvardsson, B. 1992, A&A, 261, 255

Nissen, P. E., Primas, F., & Asplund, M. 2000, Oxygen Abundances in Old Stars and Implications to Nucleosynthesis and Cosmology, 24th meeting of the IAU, Joint Discussion 8, August 2000, Manchester, England, 8, E21

Press, W. H., Flannery, B., P., Teukolsky, S. A., & Vetterling, W. T. 1986, Numerical Recipes (Cambridge: Cambridge Univ. Press)

Reetz, J. 1999a, PhD Dissertation, Ludwig-Maximilians Universität, München

Reetz, J. 1999b, Ap&SS, 265, 171

Rolleston, W. R. J., Smartt, S. J., Dufton, P. L., & Ryans, R. S. I. 2000, A&A, 363, 537

Sauval, A. J., Grevesse, N., Zander, R., Brault, J. W., & Stokes, G. M. 1984, ApJ, 282, 330

Stein, R. F. & Nordlund, A. 1998, ApJ, 499, 914

Storey, P. J., & Zeippen, C. J. 2000, MNRAS, 312, 813

Sugar, J., & Corliss, C. 1985, J. Phys. Chem. Ref. Data 14, Suppl. No. 2

Takeda, Y. 1994, PASJ, 46, 53

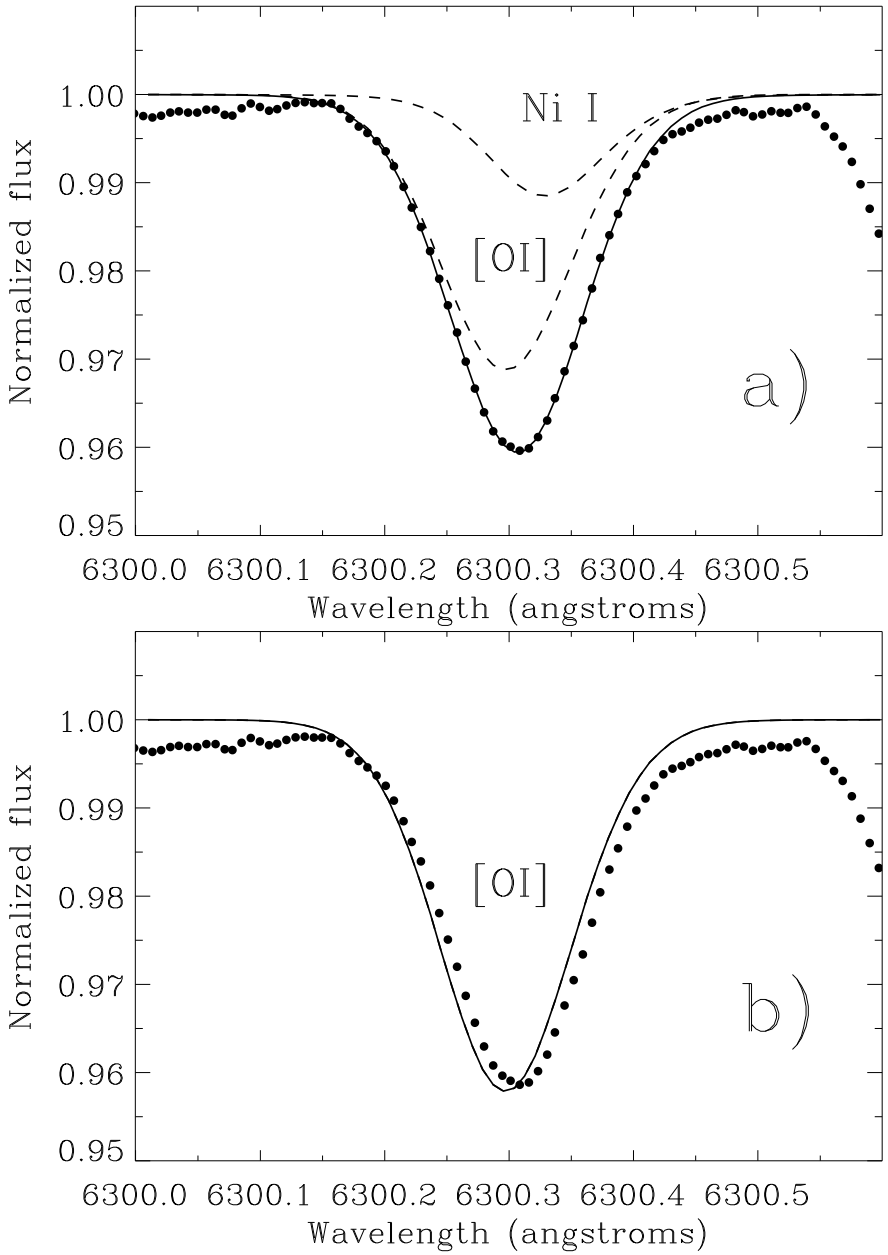

Fig. 1.— a) Comparison between the observed (filled circles) and synthetic (solid line) profiles after the χ^2 minimization. The individual calculations of the oxygen and nickel lines are also shown with dashed lines. b) Best fit assuming the observed feature is entirely produced by the oxygen forbidden line.

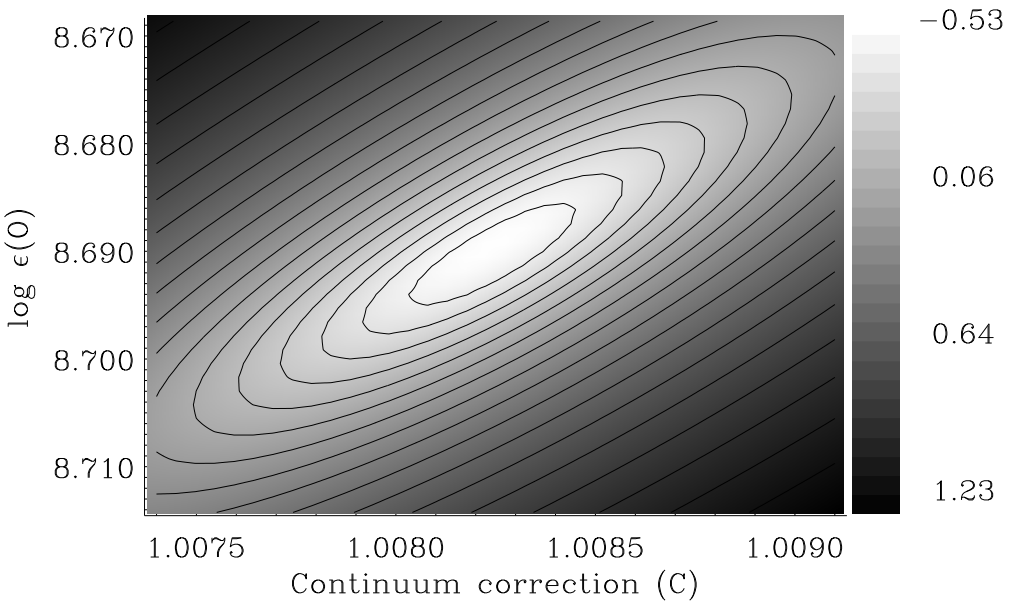

Fig. 2.— Contour and gray-scale plot showing the variation of the reduced χ^2 as a function of the continuum level and the oxygen abundance, while keeping the nickel abundance constant. The plot uses logarithmic units, and therefore the units in the code bar of the gray-scale are dex.